Received: 7 February 2022 | Revised: 28 May 2022 | Accepted: 27 July 2022

DOI: 10.1002/cac2.12348

CANCER COMMUNICATIONS Open Access

ORIGINAL ARTICLE

Pivotal roles of tumor-draining lymph nodes in the abscopal effects from combined immunotherapy and radiotherapy

Zhaoyun Liu[1,2,3,†] | **Zhiyong Yu**[3,†] | **Dawei Chen**[1,2,†] | **Vivek Verma**[4] | **Chenxi Yuan**[2] | **Minglei Wang**[1,2] | **Fei Wang**[1,2] | **Qing Fan**[5] | **Xingwu Wang**[1,2] | **Yang Li**[1,2] | **Yuequn Ma**[1,2] | **Meng Wu**[1,2] | **Jinming Yu**[1,2,6]

[1]Department of Oncology, Shandong University Cancer Center, Jinan, Shandong 250117, P. R. China

[2]Department of Radiation Oncology and Shandong Provincial Key Laboratory of Radiation Oncology, Shandong Cancer Hospital and Institute, Shandong First Medical University and Shandong Academy of Medical Sciences, Jinan, Shandong 250117, P. R. China

[3]Breast Cancer Center, Shandong Cancer Hospital and Institute, Shandong First Medical University and Shandong Academy of Medical Sciences, Jinan, Shandong 250117, P. R. China

[4]Department of Radiation Oncology, The University of Texas MD Anderson Cancer Center, Houston, Texas 77030, United States

[5]Department of Pharmacy, Shandong Cancer Hospital and Institute, Shandong First Medical University and Shandong Academy of Medical Sciences, Jinan, Shandong 250117, P. R. China

[6]Research Unit of Radiation Oncology, Chinese Academy of Medical Sciences, Jinan, Shandong 250117, P. R. China

Correspondence
Jinming Yu and Meng Wu, Shandong Cancer Hospital and Institute, Shandong First Medical University and Shandong Academy of Medical Sciences, Jinan 250117, Shandong, P. R. China
Email: sdyujinming@163.com, wumeng7777@163.com

Abstract

Background: Currently, due to synergy enhancement of anti-tumor effects and potent stimulation of abscopal effects, combination therapy with irradiation and programmed cell death protein 1/programmed death-ligand 1 (PD-1/PD-L1) immune checkpoint inhibition (immuno-radiotherapy, iRT) has revolutionized the therapeutic guidelines. It has been demonstrated that tumor-draining lymph nodes (TDLN) are essential for effective antitumor immunity induced by radiotherapy, immunotherapy, or iRT. Given that the function of TDLN in iRT remains unclear, this study aimed to investigate the function and mechanism of TDLN in iRT-induced abscopal effects.

Methods: The function of TDLN was evaluated using unilateral or bilateral MC38 and B16F10 subcutaneous tumor models with or without indicated

List of abbreviations: cGAS-STING, the cyclic GMP-AMP synthase-stimulator of interferon genes; DAPI, 4′,6′-diamidino-2-phenylindole; DC, dendritic cell; DMEM, Dulbecco's modified Eagle's medium; DPBS, Dulbecco's phosphate-buffered saline; FBS, fetal bovine serum; IFN-γ, interferon-γ; iNOS, inducible nitric oxide synthase; iRT, combination treatment with immunotherapy and radiotherapy; MHC I, major histocompatibility complex class I; M-MDSC, monocytic MDSC; PD-1, programmed cell death protein 1; PD-L1, programmed death-ligand 1; PMN-MDSC, polymorphonuclear-myeloid-derived suppressor cell; RT, irradiation; RNA-seq, RNA-sequencing; TAM, tumor-associated macrophage; TDLN, Tumor-draining lymph node; TIL, Tumor-infiltrating lymphocyte.

[†]These authors contributed equally to this work.

TDLN. The flow cytometry, multiple immunofluorescence analysis, and NanoString analysis were utilized to detect the composition and function of the immune cells in the primary and abscopal tumor microenvironment. Additionally, we tempted to interrogate the possible mechanisms via RNA-sequencing of tumor-infiltrating lymphocytes and TDLN.

Results: TDLN deficiency impaired the control of tumor growth by monotherapy. Bilateral TDLN removal rather than unilateral TDLN removal substantially curtailed iRT-stimulated anti-tumor and abscopal effects. Furthermore, in the absence of TDLN, the infiltration of $CD45^+$ and $CD8^+$ T cells was substantially reduced in both primary and abscopal tumors, and the anti-tumor function of $CD8^+$ T cells was attenuated as well. Additionally, the polarization of tumor-associated macrophages in primary and abscopal tumors were found to be dependent on intact bilateral TDLN. RNA-sequencing data indicated that impaired infiltration and anti-tumor effects of immune cells partially attributed to the altered secretion of components from the tumor microenvironment.

Conclusions: TDLN play a critical role in iRT by promoting the infiltration of $CD8^+$ T cells and maintaining the M1/M2 macrophage ratio.

KEYWORDS

immuno-radiotherapy, tumor-draining lymph node, T cells, tumor-associated macrophage

1 | BACKGROUND

Radiotherapy is generally considered as a local treatment modality, however, an increasing number of preclinical and clinical studies have demonstrated that radiotherapy could provoke systemic innate and adaptive immune responses, and could result in tumor regression outside the irradiated area in select cases, which is termed "abscopal effects" [1–3]. Despite this excitement, some patients demonstrate primary or secondary radiotherapy resistance and abscopal effects induced by radiotherapy alone are rare [4]. In recent years, immunotherapy, especially programmed cell death protein 1/programmed death-ligand 1 (PD-1/PD-L1) immune checkpoint blockades therapy, has revolutionized the treatment of various malignancies, such as non-small cell lung cancer, melanoma, and renal cancer [5, 6]. However, fewer than 50% of patients exhibit a durable antitumor response and benefit from immunotherapy alone, with a considerable proportion of patients developing resistance [7, 8]. Because radiotherapy can elicit an adaptive immune response and immune checkpoint inhibitors can enhance T cell function, combination treatment with immunotherapy and radiotherapy (immuno-radiotherapy, iRT) has been developed and attempted [9]. Accumulating clinical trials and preclinical studies have illustrated that the addition of immunotherapy significantly augments radiotherapy-induced abscopal effects, and radiotherapy may (at least partially) help to overcome immunotherapy resistance by means of increasing tumor immunogenicity and reprogramming the neoplastic microenvironment [10, 11].

The lymph node is an important secondary lymphoid organ that regulates interactions and trafficking of multiple types of immune cells, including T, B, and antigen-presenting cells [12–14]. Radiotherapy could invigorate the tumor-killing capacity of cytotoxic T cells in the tumor microenvironment, possibly by promoting major histocompatibility complex class I (MHC I) expression in tumor cells and activating the cyclic GMP-AMP synthase-stimulator of interferon genes (cGAS-STING) pathway in dendritic cells (DCs) [15, 16]; however, tumor-draining lymph nodes (TDLN) are also pivotal for radiotherapy-mediated immune stimulation and abscopal effects [17, 18]. Similarly, although PD-1/PD-L1 blockade is thought to activate T cells in the tumor microenvironment, TDLN (instead of non-TDLN) contribute to the anti-tumor effects of PD-1/PD-L1 blockade as well [19].

Phenotypically, dysfunction of TDLN caused by surgery, irradiation, pharmacological inhibitors, or genetic ablation significantly attenuates the anti-tumor effects of radiotherapy, immunotherapy and iRT [20–22]. Takeshima *et al.* [20] reported that surgical excision of TDLN attenuated the anti-tumor effects induced by irradiation with a declining proportion of cytotoxic T lymphocytes in the primary

tumor. Similarly, Marciscano *et al.* [21] demonstrated that elective TDLN irradiation reduced immune infiltration of iRT by regulating chemokine signaling, leading to the unfavorable tumor immune microenvironment in the primary tumor. However, the role of the TDLN of abscopal tumors remains unclear. In actual clinical practice, abscopal effects are rare with radiotherapy alone, while the addition of immunotherapy significantly augments abscopal effects [23–26]. Buchwald *et al.* [17] reported the important role of TDLN in abscopal effects induced by radiotherapy. Zhang *et al.* [27] reported the crucial role of TDLN in regulating local and systemic antitumor effects induced by hypofractionated radiotherapy and immune checkpoint inhibitors. However, the role of TDLN in iRT-induced abscopal effects remains unclear and warrants further investigation. Mechanically, naïve T cells are activated in TDLN by mature DCs after tumor irradiation, and the function of irradiation-induced tumor-specific cytotoxic T lymphocytes and stem-like $CD8^+$ T cells is greatly compromised in the absence of TDLN [20]. In the context of immunotherapy, T cells in TDLN are activated after PD-1 blockade treatment [19, 28], and blocking PD-L1 in TDLN generates progenitor-exhausted T cells that seed the tumor, contributing to anti-tumor effects [19, 29]. Altogether, preclinical observations have validated the essential role of TDLN.

Thus far, the vital roles of TDLN in radiotherapy, immunotherapy, and iRT have been illustrated by several studies [17, 21, 30]. Since iRT is becoming increasingly utilized in the study of metastatic cancers, the function of TDLN in iRT-induced anti-tumor effects warrants further investigation. Therefore, this study sought to evaluate iRT-induced anti-tumor and abscopal effects in a murine model with surgically removed TDLN.

2 | MATERIALS AND METHODS

2.1 | Mice and cell lines

Female C57BL/6J mice (age, 6-8 weeks) were purchased from Beijing Huafukang Biosciences Corporation (Beijing, China). Experiments involving animals were reviewed and approved by the Shandong Cancer Hospital according to Institute Animal Care and Use Committee guidelines (Permit number: SDTHEC2020001013). The mice were bred and maintained in our air-conditioned animal facility and housed in a climate-controlled (temperature = 24°C; humidity = 40%-60%) light-regulated room with a 12/12 h light/dark cycle and with ad libitum access to food and water. They were euthanized in a CO_2 chamber at an experimental or a humane endpoint (tumor size >1500 mm^3), whichever occurred first.

The murine colon adenocarcinoma cell line MC38 and murine melanoma cell line B16F10 were generous gifts received from the laboratory of Professor Liufu Deng from the Shanghai Institute of Immunology, Shanghai Jiaotong University School of Medicine (Shanghai, China). The MC38 cells were cultured in Dulbecco's modified Eagle's medium (DMEM; ThermoFisher, Waltham, USA) and B16F10 cells in RPMI-1640 (ThermoFisher) supplemented with 10% fetal bovine serum (FBS; ThermoFisher), 100 U/mL penicillin/streptomycin (Solarbio, Beijing, China) at 37°C with 5% CO_2.

2.2 | Subcutaneous tumor models and treatment

Unilateral or bilateral subcutaneous tumor models were established using MC38 and B16F10 cells. Briefly, C57BL/6J mice were subcutaneously inoculated with indicated tumor cells on the left flank (primary tumor: 1×10^6 MC38 cells or 5×10^5 B16F10 cells) and/or on the right flank (abscopal tumor: $0.3\text{-}0.4 \times 10^6$ MC38 cells or 3×10^5 B16F10 cells) on Day 0. After the diameter of the primary tumors reached 6-8 mm (approximately on Day 9 for MC38 tumors and on Day 7-8 for B16F10 tumors post tumor challenge), the mice were randomly allocated and subjected to various treatments. Tumors were monitored at least twice every week, and the mice were euthanized at indicated time points.

To determine the location of TDLN, methylene blue staining was performed as previously reported [31]. Briefly, 10 μL medical methylene blue injection was injected subcutaneously at the tumor site, and the mice were sacrificed and TDLN were dissected 5 min after injection. Unilateral or bilateral TDLN were surgically removed from mice on indicated days or sham surgery, and subsequently, anti-PD-1 (200 μg/mouse; #BE0146, BioXcell, West Lebanon, NH, USA) was intraperitoneally administrated to mice on the same day and every other day for a total of three times. One day after TDLN removal surgery or sham surgery, the primary tumors (on the left flank) were irradiated with one fraction of 12 Gy using the RS2000-225 Biological Irradiator (Rad Source Technologies, Inc. Buford, GA, USA), with the body of mice protected by a 4-mm-thick lead shield (Supplementary Figure S1A). Thereafter, the tumor volumes were monitored twice every week.

For in vivo depletion of $CD8^+$ T cells, tumor-bearing mice were intraperitoneally injected with anti-mouse CD8α antibody (300 μg/mouse; #BE0061, BioXcell) 2 days before irradiation and twice weekly thereafter. In addition, tumor-bearing mice were intragastrically injected with FTY720 (20 μg/mouse; #S5002, Selleck, Houston, TX, USA) 1 day before tumor-directed irradiation and every

day thereafter with a lavage needle as described previously [32]. Peripheral $CD3^+$ T cells were detected 48 h after irradiation.

The mice were euthanized at indicated time points or after the cumulative tumor burden had reached 1500 mm^3, and 60 days after tumor inoculation for $CD8^+$ T cell deletion experiments.

2.3 | Flow cytometry

Subcutaneous tumors were collected 6-7 days after tumor irradiation, minced with ophthalmic forceps, and subsequently digested with 1 mg/mL collagenase type 4 (LS004186, Worthington, New York, NY, USA) and 0.2 mg/mL Dnase I (DN25, Sigma-Aldrich, St Louis, MO, USA) at 37°C for 30 minutes. Digestion was terminated using RPMI-1640 with 2% FBS, and the solution was filtered using a 70 μm cell strainer (Corning, New York, NY, USA) to obtain single cell suspensions, followed by cell staining and flow cytometry. For surface staining, the single cell suspensions were incubated with anti-mouse CD16/CD32 antibody (1:50; #553141, BD Biosciences, Franklin Lakes, NJ, USA) for 15 minutes at 4°C to block nonspecific antibody binding, washed with FACS buffer (2% FBS in PBS), and subsequently stained with an antibody cocktail against CD45.2 (1:200; #109839, Biolegend, San Diego, CA, USA), Ly6C (1:200; #128035, Biolegend), Ly6G (1:200; #127643, Biolegend), CD11b (1:200; #101216, Biolegend), F4/80 (1:200; #123137, Biolegend), CD11c (1:200; #117310, Biolegend), MHC-II (1:200; #107625, Biolegend), CD86 (1:200; #553691, BD Biosciences), CD206 (1:200; #141706, Biolegend), CD8 (1:200; #100730 or #100753, Biolegend), and Fixable Viability Stain 780 (1:1000; #565388, BD Biosciences). For intracellular staining and evaluating the function of T cells in the tumor microenvironment, the single cell suspensions were treated with Cell Activation Cocktail (with Brefeldin A) (1:200; #423304, Biolegend) for 4 h before cell staining and stained with an antibody cocktail against CD45.2 (1:200; #109839, Biolegend) and CD8 (1:200; #100730 or #100753, Biolegend), The samples were fixed in fixation/permeabilization buffer (#562574, BD Biosciences) at 4°C for 1 h, washed with 1 × permeabilisation/wash buffer and incubated with the corresponding antibody cocktails including Granzyme B (1:200; #372204, Biolegend), and interferon-γ (IFN-γ,1:200; #505831, Biolegend) in permeabilization buffer in the dark at 4°C for 40-60 minutes. Flow cytometry was performed on an LSR Fortessa system (BD Biosciences), and the output was analyzed using the FlowJo software (version 10.4, TreeStar, Ashland, OR). $CD8^+$ T cells were identified as $CD45^+$ $CD8^+$. IFN-γ^+ and Granzyme B^+ were used to define the cytotoxic function of $CD8^+$ T cells. M1 tumor-associated macrophages (TAMs) were identified as $CD45^+Ly6C^{low}Ly6G^{low}CD11b^+F4/80^+CD86^+$ or $CD45^+Ly6C^{low}Ly6G^{low}CD11b^+F4/80^+$ $MHCII^+$, and M2 TAM were identified as $CD45^+Ly6C^{low}Ly6G^{low}$ $CD11b^+F4/80^+$ $CD206^+$.

2.4 | RNA-sequencing (RNA-seq) and NanoString analysis

Single cell suspensions (prepared as mentioned above) were obtained 7 days after tumor irradiation. Tumor-infiltrating lymphocytes (TILs) were isolated via density gradient centrifugation using Ficoll (17-5442-02, GE Healthcare, Pittsburgh, PA, USA) as described previously [33]. Briefly, single cells were resuspended in 4 mL of Dulbecco's phosphate-buffered saline (DPBS; Solarbio, Beijing, China) and transferred to a 15 mL tube; subsequently, 2 mL of Ficoll was slowly pipetted on the bottom, and all samples were then centrifuged at 2000 rpm at 20°C for 20 minutes with no brake and acceleration. Cells in the interphase were collected, washed and subjected to RNA-seq. The total RNA of TILs was extracted using the RNeasy Mini Kit (Qiagen, Hilden, Germany). RNA libraries were prepared using the VAHTS mRNA-seq v2 Library Prep Kit (Vazyme, Nanjing, China), and sequencing was performed on the NovaSeq 6000 platform (Berry Genomics Co., Ltd. Beijing, China). Pathway analysis was performed via KEGG software. RNA-seq reads were aligned to NanoString of 770 immune-related genes and analyzed using the nCounter® analysis system (Fynn Biotechnologies Ltd, Jinan, China).

2.5 | H&E staining and Immunofluorescence staining

TDLN were surgically removed from C57BL/6J mice, formalin-fixed and embedded in paraffin. For H&E staining, sections were processed by dewaxing, hydration, dyeing, dehydration, and sealing.

Tumor tissues were obtained 7 days after tumor irradiation, fixed in formalin, and embedded in paraffin. Immunofluorescence staining was performed according to the manufacturer's instructions (Opal™ 7-Color Manual IHC Kit; NEL811001KT, Akoya Biosciences, Marlborough, MA, USA). Briefly, paraffin sections were incubated with sodium citrate for 10-25 minutes for antigen retrieval, blocked using BF block buffer containing 30%-40% goat serum for 1 h at room temperature, and subsequently incubated with primary antibodies against F4/80 (1:200; 70076, Cell Signaling Technology, Danvers, MA, USA, marker of mouse monocytes/macrophages), inducible nitric oxide

synthase (iNOS, 1:200; ab3523, Abcam, Cambridge, MA, USA, a marker of mouse M1 TAM), CD206 (1:200; ab64693, Abcam, a marker of mouse M2 TAM), CD45 (1:200; 20103-1-AP, Proteintech, Chicago, IL, USA), and CD8 (1:200; 98941, Cell Signaling Technology) at room temperature for 2 h or 4°C overnight with an additional incubation of 0.5-2 h at room temperature. Thereafter, the sections were incubated with secondary antibodies (1 ×, ARH1001EA, Akoya Biosciences, Marlborough, MA, USA) for 10 minutes followed by incubation with appropriate opal fluorophore reagents at room temperature for 10 minutes. Finally, the sections were stained with 4′,6′-diamidino-2-phenylindole (DAPI) for 7 minutes at room temperature; and $CD45^+CD8^+$ T cells, $F4/80^+iNOS^+$ cells (M1 TAM) and $F4/80^+CD206^+$ cells (M2 TAM) were photographed and analyzed on a Vectra Polaris system (Akoya Biosciences).

2.6 | Statistical analysis

Representative data were obtained from 2-3 independent experiments and are expressed as mean ± standard error (SE). Survival graphs were analyzed using the Kaplan-Meier method and compared using the log-rank tests. Two-way ANOVA was used for tumor growth comparison, and one-way ANOVA for multiple groups comparison, and all were followed by Tukey's multiple comparison test. $P < 0.05$ was considered to be statistically significant. All statistical analyses were performed using the GraphPad Prism software (v8.0.2; La Jolla, CA, USA).

3 | RESULTS

3.1 | Intact TDLN are essential for iRT-induced anti-tumor and abscopal effects

To examine the function of TDLN, methylene blue staining was performed in vivo to determine the location of TDLN in the tumor models. The location of TDLN was similar to that reported previously [21]. Subsequently, H&E staining of the surgically removed tissue revealed typical lymphoid nodal structure (Supplementary Figure S1B), indicating that TDLN were successfully removed from the mouse models when indicated.

To verify the hypothesis that TDLN were important for iRT, mice with unilateral subcutaneous tumors were subjected to either monotherapy (irradiation or anti-PD-1 treatment) or combinatorial iRT in the presence or absence of the corresponding TDLN (Figure 1A). Compared with radiotherapy or anti-PD-1 therapy, iRT augmented anti-tumor effects in both MC38 and B16F10 tumor models. Moreover, intact TDLN were required for iRT-induced anti-tumor effects (Figure 1B-C, Supplementary Figure S1C). Furthermore, administration of FTY720, which can block T cell egress from lymphoid tissues, dramatically decreased the proportion of peripheral T cells and eliminated iRT-induced anti-tumor effects (Figure 1D-G, Supplementary Figure S1D-E). Therefore, TDLN functioned as essential hubs of anti-tumor responses induced by iRT.

As previously reported, compared with radiotherapy, iRT dramatically stimulated abscopal effects, which requires adequate adaptive immune responses [34]. We next interrogated whether iRT-stimulated abscopal effects also require TDLN and found that a single fraction of 12 Gy on a primary tumor with systemic administration of anti-PD-1 antibody induced dominant abscopal effects in the bilateral subcutaneous tumor models (Supplementary Figure S1F). To further determine the functions of the TDLN of primary and abscopal tumors, unilateral or bilateral TDLN were surgically removed before anti-PD-1 administration and irradiation, and the contribution of TDLN to anti-tumor and abscopal effects induced by different treatments varied (Supplementary Figure S2A). Resection of unilateral or bilateral TDLN alone did not affect tumor growth (Supplementary Figure S2B), and it seemed that TDLN slightly influenced the anti-tumor effects induced by anti-PD-1 monotherapy (Supplementary Figure S2C). However, intact TDLN of the primary tumors (instead of the abscopal tumors) were found to be essential for irradiation monotherapy-induced primary and secondary tumor regression (Supplementary Figure S2D), and bilateral (instead of unilateral) TDLN deficiency dramatically attenuated iRT-stimulated abscopal effects (Figure 1H, Supplementary Figure S2E). In all, these results suggested that TDLN were essential for iRT-induced anti-tumor effects, and intact TDLN of both primary and abscopal tumors were essential for iRT-induced abscopal effects.

3.2 | Transcriptomes of TILs in iRT-treated primary and abscopal tumors demonstrate different repertoires after removal of bilateral TDLN

iRT-induced abscopal effects depend on adequate innate and adaptive immune responses, which are executed by immune cells in the tumor microenvironment. Therefore, to evaluate the impact of iRT on TILs, TILs were isolated from iRT-treated primary and abscopal tumors 7 days after irradiation and subjected to RNA-seq. TILs, isolated from either primary or abscopal tumors, showed distinct transcriptomes after iRT and subsequent TDLN

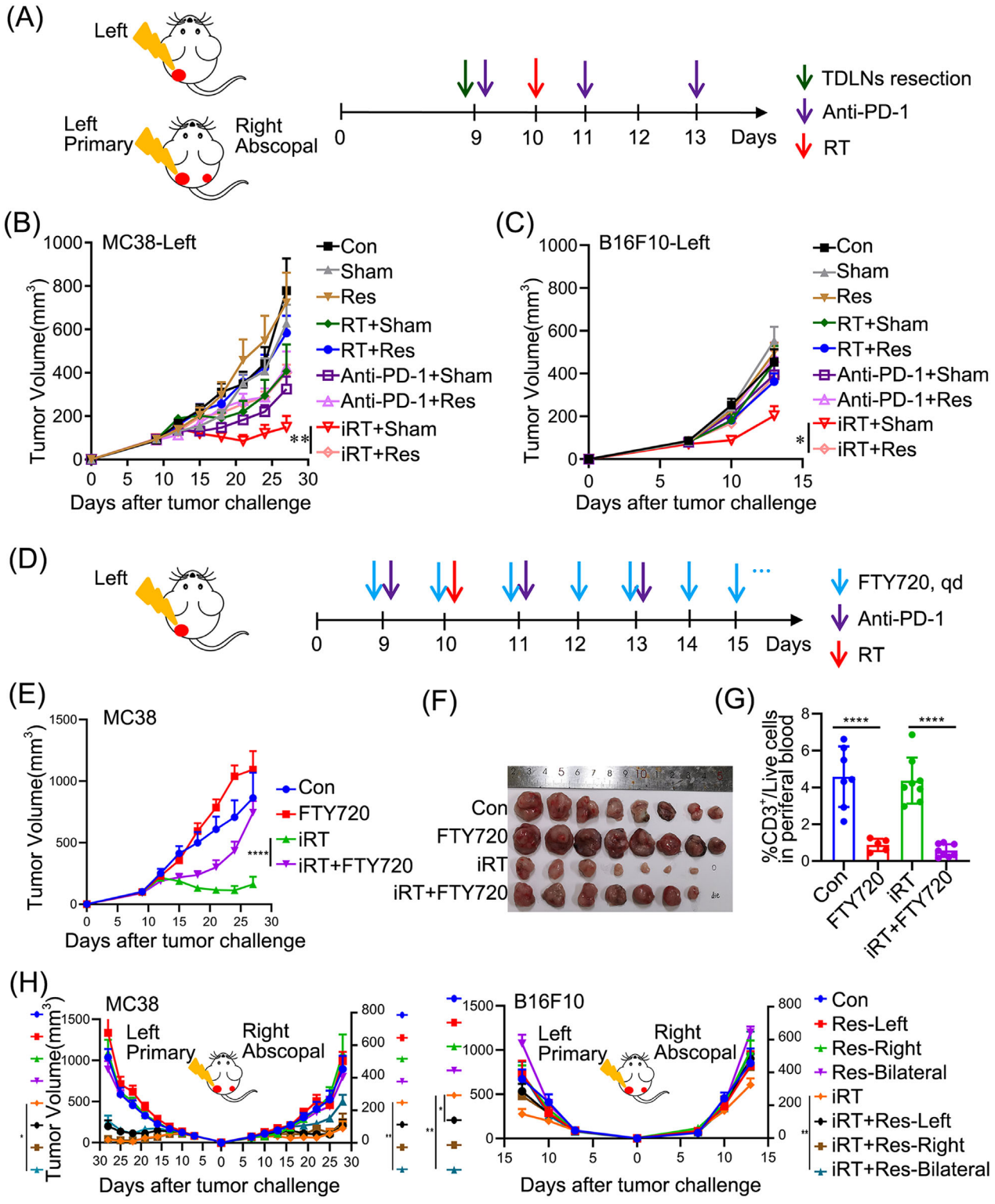

FIGURE 1 **TDLN are essential for anti-tumor and abscopal effects induced by iRT**. (A) Schematic diagrams of unilateral and bilateral subcutaneous tumor models. **(B-C)** Tumor volumes of the unilateral MC38 (B) and B16F10 (C) tumor models treated as Panel A. **(D)** Schematic diagrams of FTY720 administration. **(E-F)** Tumor volumes (E) and representative images (F) of isolated MC38 tumors treated with iRT with or without FTY720 treatment. **(G)** The proportion of $CD3^+$ T cells in peripheral blood in mice treated with or without FTY720. **(H)** Tumor volumes of the bilateral MC38 and B16F10 tumor models treated as Panel A. Representative data were obtained from 2-3 independent experiments. Data are expressed as mean ± SEM (n = 6-9 per group).*, $P < 0.05$; **, $P < 0.01$; ****, $P < 0.0001$. Abbreviations: TDLN, Tumor-draining lymph nodes; PD-1, programmed cell death protein 1; SEM, standard error of the mean; Con, control; Sham, sham surgery; Res, resection; RT, radiotherapy; iRT, combination of radiotherapy and anti-PD-1; Res-Left, removal of TDLN on the left side; Res-Right, removal of TDLN on the right side; Res-Bilateral, removal of TDLN on both sides.

removal (Figure 2A). Analysis of differentially expressed genes showed that several genes were downregulated after bilateral TDLN removal in the context of iRT in both primary and abscopal tumors when compared with the iRT group (Figure 2B). For example, *Pydc4*, *Rhov*, *Oasl1*, *Hdc*, *Isg15*, *Il1f9*, *Saa3*, *Ccl4*, *Treml2*, *H2-Q10*, and *Cebpe* in primary tumors and *Ly6c2*, *CD8b1*, *Gimap5*, *Lat*, *Hcst*, *Cd3d*, *Pglyrp1*, *Tusc5* and *H2-Q10* in abscopal tumors were significantly downregulated with the absence of TDLN. Because most of these genes are associated with T cell function [35–38], the finding indicated that the removal of bilateral TDLN might lead to impaired iRT-induced T cell responses.

Next, we further compared the pathways enriched in the iRT group *vs*. control group with those enriched in the iRT group *vs*. the group with iRT treatment combined with TDLN removal in primary tumors. Two overlapping pathways were found, one related to cytokine-cytokine receptor interaction and the other to phagosome (Figure 2C-D). Using similar comparison methods to examine the TILs of abscopal tumors, 9 overlapping pathways were found, including those related to the cytokine-cytokine receptor pathway and phagosome in addition to the chemokine signaling pathway (Figure 2C-D). Moreover, the genes downregulated in the absence of TDLN were also enriched in the pathways mentioned above. Of note, metabolic and oxidative phosphorylation pathways were significantly upregulated in the TILs of abscopal tumors after iRT, which were downregulated after TDLN removal, thus indicating a potential difference between the primary and abscopal tumor microenvironment (Figure 2C).

Furthermore, we examined the transcriptome of bilateral TDLN 1, 3, 5 and 7 days after iRT. Differentially expressed genes and enriched pathways in the TDLN of primary and abscopal tumors indicated that the TDLN of primary and abscopal tumors might contribute to antitumor immune responses through different mechanisms in a time-dependent manner (Supplementary Figure S3). In addition, the *Thbs4* gene (associated with stem cell differentiation) was found to be significantly upregulated in the iRT groups *vs*. control groups in both primary and abscopal tumors. Tumor-reactive stem-like TILs are associated with complete cancer regression, and TDLN may be the source of stem-like cells in tumors [39, 40].

3.3 | TDLN removal impairs iRT-induced anti-tumor immune responses mediated by $CD8^+$ T cells

Owing to the importance of $CD8^+$ T cells as "effector cells" for iRT-mediated immune responses and as indicated by the RNA-seq data (Figure 2B), we assessed whether TDLN promoted iRT-induced anti-tumor and abscopal effects via the filtration and function of $CD8^+$ T cells in the tumor microenvironment. We first utilized the unilateral MC38 tumor models, which were subjected to irradiation and/or anti-PD-1 administration in the presence or absence of TDLN. Tumors were collected 7 days post irradiation, and the immune microenvironment was analyzed via flow cytometry using the gating strategy (Supplementary Figure S4). The results revealed that TDLN removal adversely affected iRT-induced $CD45^+$ and $CD8^+$ T cell infiltration, and monotherapy-stimulated $CD45^+$ and $CD8^+$ T cell infiltration was slightly altered by TDLN removal (Supplementary Figure S5A). These results suggested that iRT-induced $CD8^+$ T cell infiltration relied on intact TDLN. Furthermore, bilateral MC38 tumor models were established and subjected to iRT treatment with or without bilateral TDLN removal. TDLN removal alone did not affect $CD45^+$ and $CD8^+$ T cell infiltration in either the primary or abscopal tumor microenvironment without iRT treatment. iRT treatment significantly increased the infiltration of $CD8^+$ and $CD45^+$ T cells, which were substantially reversed by bilateral TDLN removal (Figure 3A-B). Furthermore, the effects of TDLN removal on the function of $CD8^+$ T cells (in the primary and abscopal tumor microenvironment) were examined. The results showed that iRT resulted in significant enrichment of IFN-γ^+ and Granzyme B^+ $CD8^+$ T cells, which was diminished after bilateral TDLN removal (Figure 3C-F). To visualize the distribution of $CD45^+$ and $CD8^+$ T cells in primary and abscopal tumors, multiplex immunofluorescence staining was utilized, and evident enrichment of $CD45^+$ and $CD8^+$ T cells were detected after iRT. However, bilateral TDLN removal attenuated this phenomenon (Figure 4A).

Additionally, to verify the involvement of $CD8^+$ T cells in iRT-stimulated abscopal effects, the anti-CD8 neutralizing antibody was used in bilateral MC38 tumor models. The results revealed that $CD8^+$ T cell depletion inhibited anti-tumor effects in both primary and abscopal tumors with compromised survival outcomes (Figure 4B-C). Altogether, these findings suggest that TDLN-mediated $CD8^+$ T cell infiltration and function are essential for iRT-induced abscopal effects.

3.4 | TDLN maintain TAM polarization in the primary and abscopal tumor microenvironment after iRT

As shown in Figure 2B, transcriptomic analysis showed that *Chil1*, *Hcar2*, *Irf7*, and *Ccl3* (primary tumors) along with *Treml2*, *Cd209a*, and *Runx1t1* (abscopal tumors) were significantly downregulated with the absence of TDLN. Because these genes are associated with macrophage

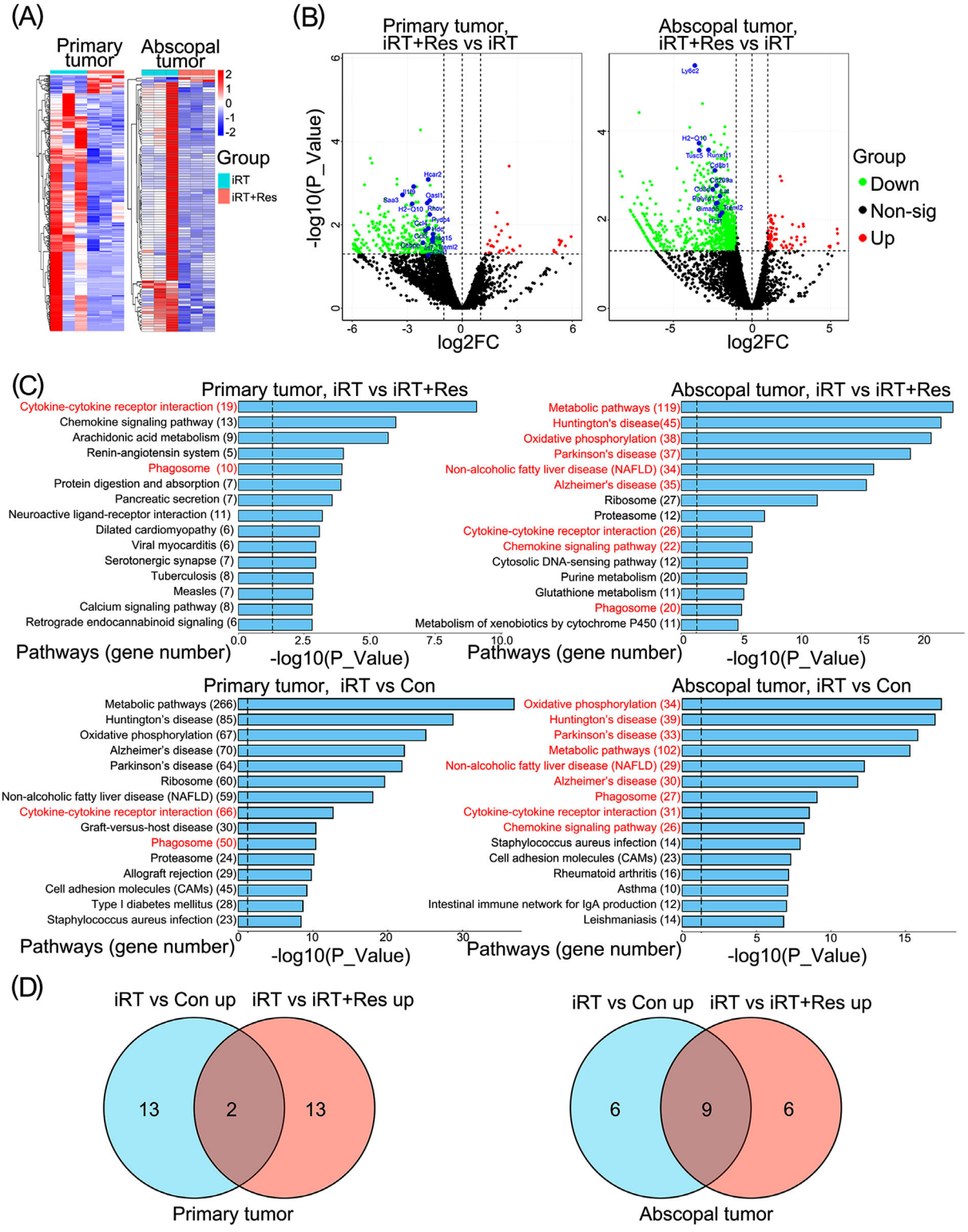

FIGURE 2 **Immune response related genes and pathways enriched in tumors treated with iRT are altered in the absence of TDLN**. (A) Heat-map demonstrating differently expressed genes in TILs isolated from primary and abscopal tumors treated with iRT in the presence or absence of bilateral TDLN (based on RNA-seq data). **(B)** Volcano plot demonstrated significantly differentially expressed genes in TILs isolated from primary or abscopal tumors treated with iRT in the presence or absence of bilateral TDLN. **(C)** KEGG pathway analysis (based on RNA-seq data) showing the top 15 pathways upregulated in TILs isolated from primary and abscopal tumors subjected to iRT in the presence or absence of bilateral TDLN. **(D)** Venn diagrams demonstrated the top 15 upregulated pathways in the iRT *vs*. Con group and iRT *vs*. iRT + Res group of primary and abscopal tumors ($n = 3$ for each group). Abbreviations: TDLN, Tumor- draining lymph nodes; TIL, Tumor-infiltrating lymphocytes; iRT, combined immunotherapy and radiotherapy; Res, bilateral TDLN resection; iRT + Res, iRT with bilateral TDLN resection; RNA-seq, RNA-sequencing; FC, fold change; non-sig, non-significant.

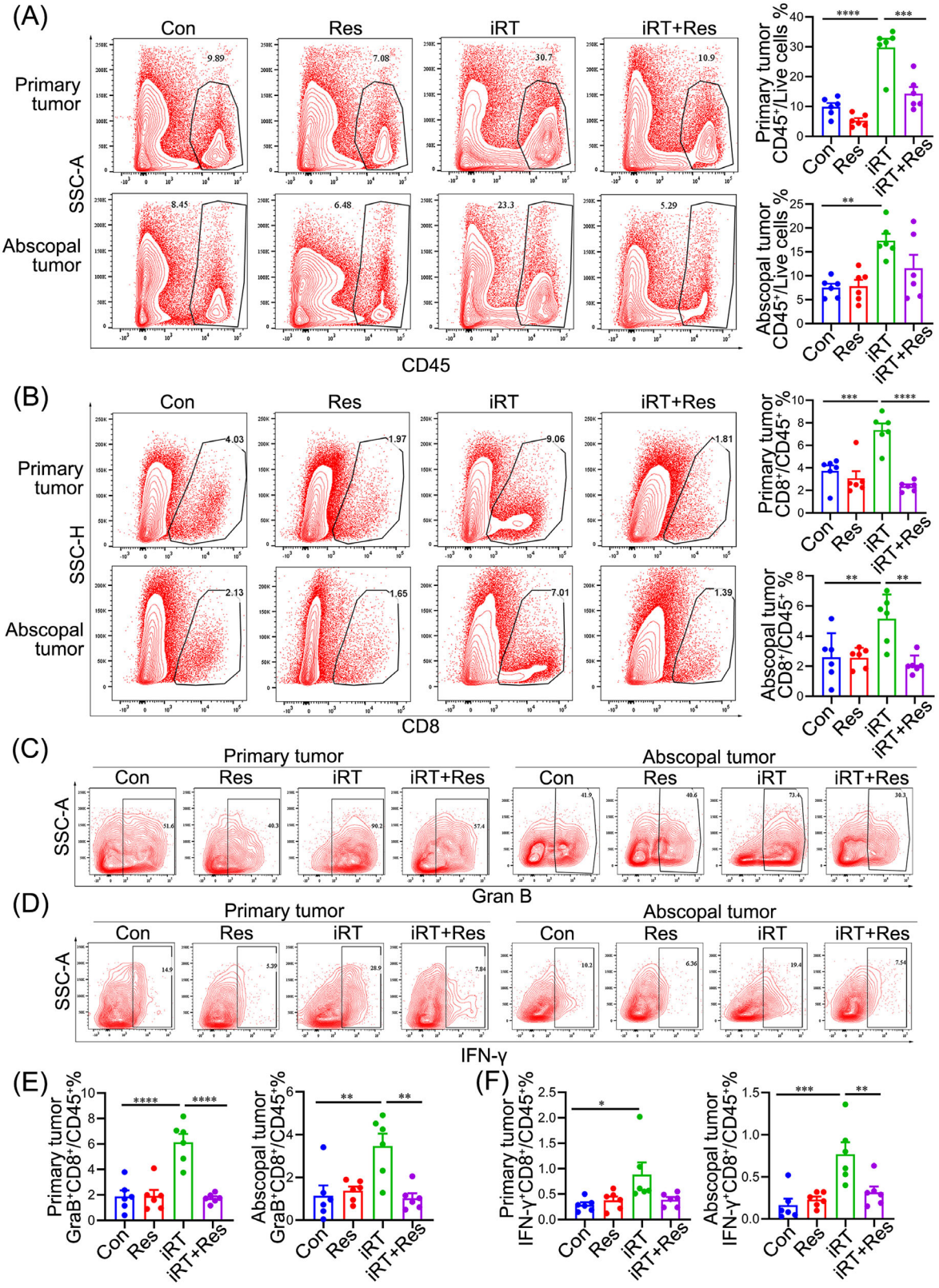

FIGURE 3 **TDLN removal abrogates iRT-induced anti-tumor immune responses**. Primary and abscopal tumors were collected and subjected to flow cytometric analysis. Representative data and quantitative analysis of $CD45^+$ cells (A) and $CD8^+$ T cells (B) isolated from primary and abscopal tumors. Representative data and quantitative analysis of Granzyme B^+ (C, E) and IFN-γ^+ (D, F) $CD8^+$ T cells isolated from primary and abscopal tumors. Representative data are obtained from 2-3 independent experiments. Data are expressed as mean ± SEM (n = 5-6 per group). *, $P < 0.05$; **, $P < 0.01$; ***, $P < 0.001$; ****, $P < 0.0001$. Abbreviations: TDLN, Tumor- draining lymph nodes; SEM, standard error of the mean; IFN-γ, interferon-γ; Con, control; Res, resection; iRT, combined immunotherapy and radiotherapy; iRT + Res, iRT with bilateral TDLN resection.

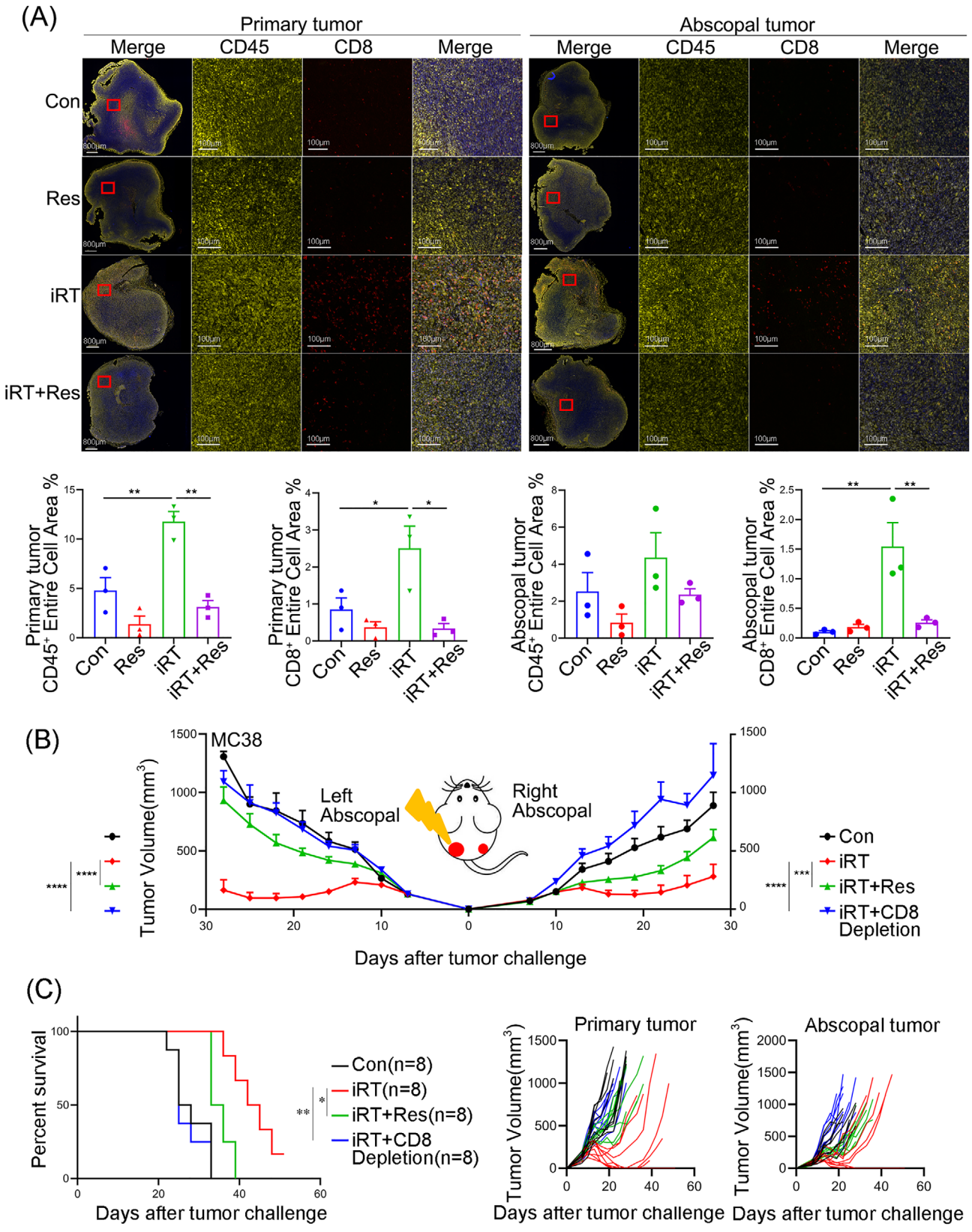

FIGURE 4 **Indispensable role of CD8$^+$ T cells in iRT-induced abscopal effects relies on intact TDLN**. (A) Multiplex immunofluorescence staining for quantitative analysis of CD45$^+$ and CD8$^+$ T cells isolated from primary and abscopal tumors of MC38 mouse models. **(B, C)** Tumor volumes (B), survival curve and tumor growth curve (C) of the bilateral MC38 models. Representative data are shown from two independent experiments. Data are expressed as mean ± SEM (n = 3-8 per group). *, P < 0.05, **, P < 0.01, ***, P < 0.001, ****, P < 0.0001. Abbreviations: TDLN, Tumor- draining lymph node; SEM, standard error of the mean; Con, control; Res, resection; iRT, combined immunotherapy and radiotherapy; iRT + Res, iRT with bilateral TDLN resection.

enrichment and function [41, 42], it was hypothesized that TAM might be affected by TDLN deficiency. Bilateral tumor models were utilized herein. Compared with the control group, the iRT group had significant infiltration of polymorphonuclear-myeloid-derived suppressor cells (PMN-MDSCs) and monocytic MDSCs (M-MDSCs) in the primary tumor microenvironment, which was not affected by TDLN removal (Supplementary Figure S5B). In addition, the abundance of DCs was not dramatically altered after iRT treatment with or without TDLN (Supplementary Figure S5B). However, in the abscopal tumor microenvironment, although iRT did not affect the enrichment of PMN-MDSCs, M-MDSCs, and DCs compared with the control group, TDLN removal decreased the infiltration of these immune cells (Supplementary Figure S5C). Moreover, the infiltration of TAM was decreased in both primary and abscopal tumors after iRT, and TDLN removal reversed this phenomenon (Supplementary Figure S5D). Thus, TDLN removal influenced the reprogramming of the tumor microenvironment in both primary and abscopal tumors.

Given that the proportion of TAM consistently varied in primary and abscopal tumors with iRT in the absence of bilateral TDLN, we further analyzed the polarization of TAM. Using a similar gating strategy as mentioned above (Supplementary Figure S4), we found that compared with iRT alone, iRT with TDLN removal tended to decrease the infiltration of M1 TAM in primary tumors, but differences were not statistically significant (P = 0.05, Figure 5A). Although the proportion of M2 TAM did not significantly change, the $CD86^+$M1/$CD206^+$M2 and $MHCII^+$M1/$CD206^+$M2 ratios significantly decreased after iRT with TDLN removal (Figure 5A, Supplementary Figure S5E). In abscopal tumors, iRT failed to affect the infiltration of $CD86^+$ M1 TAM, MHC-II^+ M1 TAM or $CD206^+$ M2 TAM in the presence or absence of TDLN. However, compared with Con group, iRT significantly upregulated M1/M2 ratio in the $CD86^+$ M1/$CD206^+$ M2 population in abscopal immune microenvironments, which depended on intact TDLN (Figure 5A, Supplementary Figure S5E). We then further analyzed the expression profile of M1 TAM-related genes based on the RNA-seq data using the NanoString molecular panels, and similar results were obtained. In both primary and abscopal tumors, iRT increased the expression of M1 TAM marker-related genes, whereas bilateral TDLN removal significantly reversed the increase in gene expression (Figure 5B). Additionally, to visualize the distribution and enrichment of M1 and M2 TAM in primary and abscopal tumors, multiplex immunofluorescence staining of primary and abscopal tumors was performed, and F4/80 was used to define total macrophages, whereas iNOS and CD206 were used to define M1 and M2 TAM, respectively. Consistent with the findings of flow cytometry, immunofluorescence staining revealed impaired enrichment of M1 TAM and abnormal infiltration of M2 TAM in primary and abscopal tumors after iRT with bilateral TDLN removal (Figure 5C). In summary, these results indicated that TDLN partially promoted iRT-induced abscopal effects by maintaining TAM polarization.

4 | DISCUSSION

This study revealed that bilateral TDLN partially regulated iRT-induced anti-tumor immune responses and abscopal effects by maintaining the infiltration and function of $CD8^+$ T cells and TAM polarization. iRT evoked an increase of $CD8^+$ T cells and M1 TAM in both primary and abscopal tumors with intact TDLN, leading to efficient anti-tumor effects. However, the absence of bilateral TDLN impaired the enrichment and cytotoxic capacity of $CD8^+$ T cells coupled with M2 polarization of TAM in the primary and abscopal tumor microenvironment, resulting in compromised iRT-induced tumor regression. (Figure 6).

Consistent with the findings of previous studies [43], this study revealed that iRT had more pronounced antitumor effects than radiotherapy or anti-PD-1 monotherapy in unilateral MC38 and B16F10 mouse models. The essential roles of TDLN in anti-tumor effects induced by either radiotherapy or immunotherapy alone has been previously described [33]. Similarly, in this study, mice treated with either modality increased tumor volumes/weights owing to TDLN removal. However, TDLN only partly contributed to the anti-tumor effects induced by either monotherapy or combination therapy, since compared with the control group, the monotherapy or iRT group that were deficient of TDLN showed limited tumor regression. We propose two potential reasons for this finding. First, pre-infiltrated $CD8^+$ T cells in the tumor microenvironment determine the efficiency of anti-tumoral immune responses induced by immunotherapy, and MC38 and B16F10 tumors are known to be "hot" tumors characterized by high infiltration of immune cells. Thus, pre-existing immune cells (especially $CD8^+$ T cells) may contribute to the anti-tumor effects of monotherapy or iRT. Tumor growth observed with $CD8^+$ T cell depletion verified the hypothesis mentioned above, that is, iRT-treated mice without TDLN showed less tumor regression than those with $CD8^+$ T cell depletion in both primary and abscopal tumors. Second, apart from anti-tumor immune responses, irradiation could induce direct cell death and contribute to tumor regression. The addition of systemic immunotherapy could augment radiotherapy-stimulated abscopal effects [4, 23]. In the present study, substantial iRT-induced abscopal effects were observed in both MC38 and B16F10 bilat-

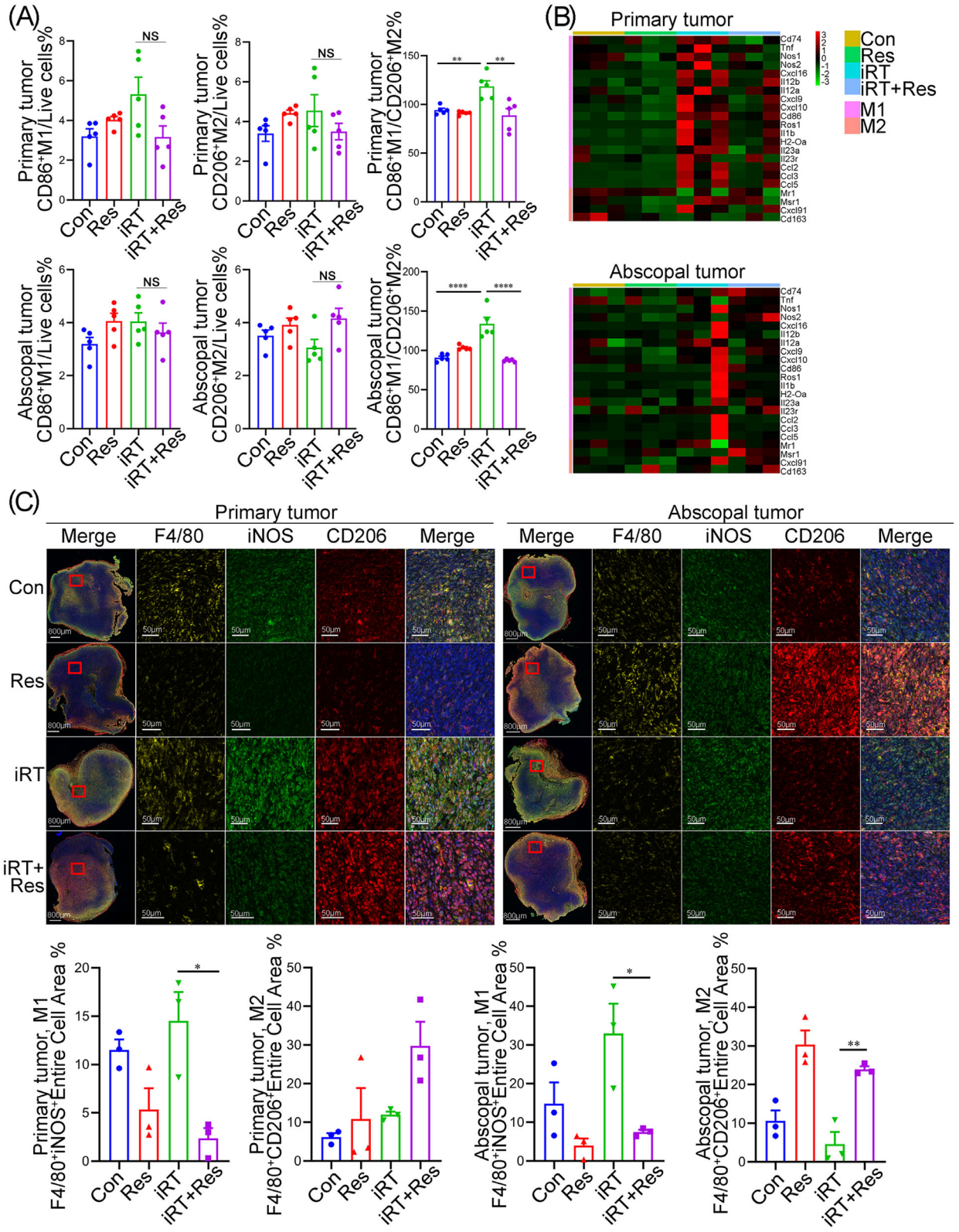

FIGURE 5 **TDLN maintains iRT-mediated TAM polarization in the primary and abscopal tumor microenvironment**. (A) Quantitative analysis of M1 and M2-like macrophages isolated from primary and abscopal tumors treated with iRT in the presence or absence of bilateral TDLN. **(B)** Heat maps demonstrating genes related to M1 or M2 macrophages in primary and abscopal tumors (NanoString molecular analysis based on RNA-seq data). **(C)** Representative images and quantitative analysis of M1-like ($F4/80^+$ $iNOS^+$) and M2-like ($F4/80^+$ $CD206^+$) macrophages in primary and abscopal tumors. Data are expressed as mean ± SEM (n = 3-7 per group). *, $P < 0.05$; **, $P < 0.01$; ***, $P < 0.001$. Abbreviations: TDLN, Tumor-draining lymph node; TAM, tumor-associated macrophage; SEM, standard error of the mean; Con, control; Res, resection; iRT, combined immunotherapy and radiotherapy; iRT + Res, iRT with bilateral TDLN resection.

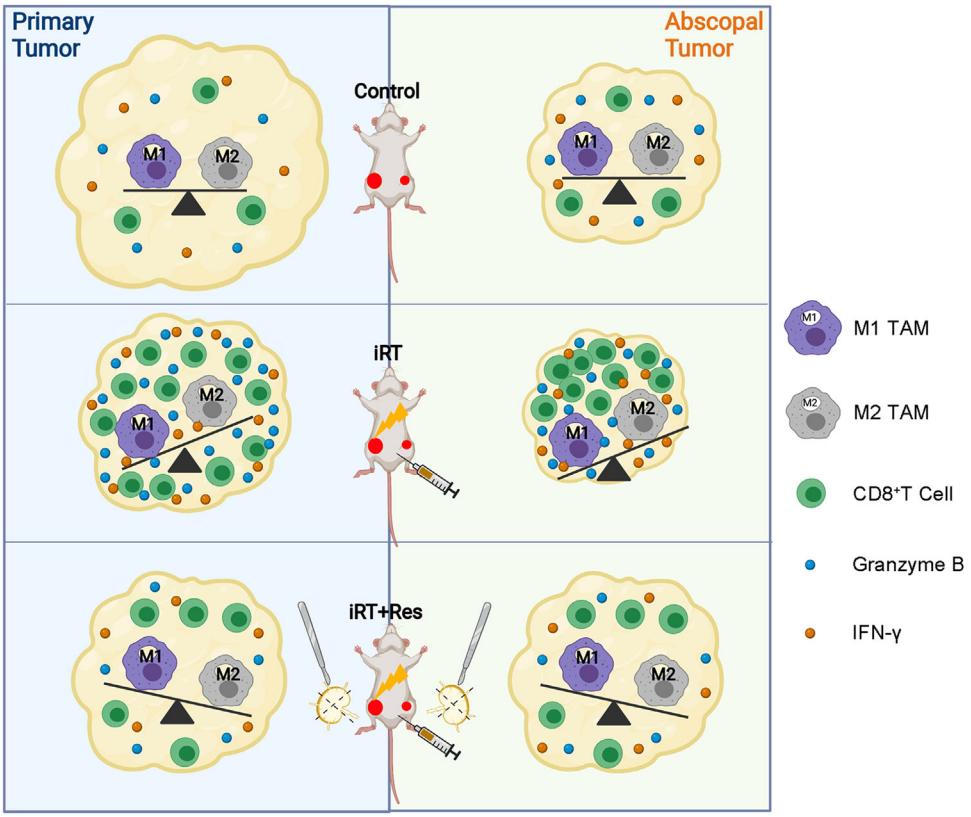

FIGURE 6 **Schematic diagram for explaining the role of TDLN in reprogramming the iRT-induced tumor immune microenvironment in both primary and abscopal tumors**. iRT lead to significant infiltration of functional $CD8^+$ T cells and M1 TAM in both primary and abscopal tumors in the presence of TDLN, leading to efficient anti-tumor effects. However, the absence of bilateral TDLN impaired the enrichment and cytotoxic capacity of $CD8^+$ T cells coupled with M2 polarization of TAM in the primary and abscopal tumor microenvironment, resulting in compromised iRT-induced tumor regression. Abbreviations: TDLN, tumor-draining lymph nodes; TAM, tumor-associated macrophage; iRT, combined immunotherapy and radiotherapy; iRT + Res, iRT with bilateral TDLN resection.

eral tumor models. To this extent, interestingly, ipsilateral TDLN removal alone exerted limited effects on iRT-treated abscopal tumor growth; only bilateral TDLN removal reversed iRT-induced abscopal tumor regression. Anti-PD-1/PD-L1 could directly lead to the release of T cells in TDLN, and TDLN of primary tumors are important sites for T cell activation via DCs from the irradiated tumor microenvironment. The unilateral removal of TDLN may be incompetent to impair iRT-induced abscopal effects. Hence, the role of contralateral TDLN in stimulating abscopal responses provides a clinical basis for sparing them from radiotherapy (or dissection), since ipsilateral TDLN are addressed with radiotherapy or surgery in most clinical circumstances. Abscopal tumor regression depends on adequate adaptive anti-tumor immunity. Therefore, TDLN are essential for anti-tumor and abscopal effects induced by iRT.

$CD8^+$ T cells are vital mediators of antitumor effects [44]. Herein, bilateral TDLN removal significantly attenuated the infiltration and cytotoxic function of $CD8^+$ T cells in iRT-treated primary and abscopal tumor microenvironment, which may partially explain the role of TDLN resection in attenuating anti-tumor effects. Noticeably, the function (and infiltration) of $CD8^+$ T cells was highly attenuated after iRT with TDLN removal, although the iRT-treated primary and abscopal tumors still showed mild tumor regression even after bilateral TDLN removal. As previously reported, $CD8^+$ T cells can be activated by antigen-presenting cells as well as anti-PD-1 in TDLN [19, 45] and subsequently migrate to the tumor microenvironment with the help of specific cytokines [46]. In addition to pre-infiltrated $CD8^+$ T cells in the tumor microenvironment, $CD8^+$ T cells may also migrate from other immune organs or peripheral circulation, so less chemokine production from the primary or abscopal tumor microenvironment, as demonstrated based on the RNA-seq data in this study, may contribute to impaired infiltration of both $CD45^+$ and $CD8^+$ T cells. It has demonstrated tumor antigen-specific $CD8^+$ T cells are the main mediators and perform important functions in the reg-

ulation of anti-tumor cellular immune responses during iRT [27, 47]. However, the infiltration and function of tumor antigen-specific $CD8^+$ T cells were not detected in this study; therefore, it cannot be negated that tumor antigen-specific $CD8^+$ T cells in iRT-treated tumor after TDLN removal may demonstrate a different trend. In all, TDLN may maintain $CD8^+$ T cell-mediated anti-tumor immunity.

TAM play an important role in modulating tumor immune responses. In this study, the M1/M2 TAM ratio was found to be decreased in primary and abscopal tumors in the absence of TDLN. To date, most studies have focused on the adaptive immune compartments, yet the contribution of other immune subsets to antitumor immunity warrants further investigation [48]. Cytokines, chemokines and cellular components in the tumor microenvironment largely determine the repertoire of TAM, which in turn exert adverse or positive effects on anti-tumor immune responses via cell-cell contact or secretion [49]. It is hypothesized that TDLN removal may facilitate the formation of an immunosuppressive microenvironment in both primary and abscopal tumors, and may consequently alter the repertoire of TAM, which in turn suppresses the anti-tumor immunity. In this study, RNA-seq of primary and abscopal TILs and TDLN illustrated different results, indicating that the underlying mechanisms may be different between primary and abscopal tumors.

Although the importance of the TDLN in iRT is revealed in this study, further details of the molecular mechanism how the TDLN maintain T cell infiltration and TAM polarization are still not clear. In addition, our studies were derived from animal experiments and lacked validation of detailed clinical data, which will be needed to assess the relevance between the survival with or without TDLN while received iRT. Further clinical studies are required.

5 | CONCLUSIONS

This study highlights the critical role of TDLN as a key orchestrator of abscopal responses mediated by combined immunotherapy and radiotherapy. This finding requires corroboration but provides a strong rationale for developing therapeutic strategies of preserving uninvolved TDLN.

DECLARATIONS

ACKNOWLEDGEMENTS

The authors thank Professor Liufu Deng from Shanghai Institute of Immunology for cell lines and Fynn Biotechnologies Ltd. for analyzing immune cell infiltration.

FUNDING

The study was supported by funding from the Academic Promotion Program of Shandong First Medical University (2019ZL002), Research Unit of Radiation Oncology, Chinese Academy of Medical Sciences (2019RU071), the foundation of National Natural Science Foundation of China (81627901, 81972863, 82030082 and 31900649), the foundation of Natural Science Foundation of Shandong (ZR201911040452 and ZR2019LZL018), the Cancer Prevention and Treatment Joint Fund of Natural Science Foundation of Shandong Province (ZR2020LZL014).

COMPETING INTERESTS

The authors declare that they have no competing interests.

AUTHOR CONTRIBUTIONS

Zhaoyun Liu and Dawei Chen: performed the experiments and wrote the manuscript. Zhiyong Yu and Vivek Verma: scientific guidance and manuscript editing. Chenxi Yuan, Fei Wang, Qing Fan, Xingwu Wang, and Yang Li performed the experiments. Minglei Wang and Yuequn Ma analyzed the data. Meng Wu and Jinming Yu: scientific guidance and resources, manuscript editing. All authors read and approved the final manuscript.

AVAILABILITY OF DATA AND MATERIALS

The datasets used and analyzed in this study are available from the corresponding author on reasonable request.

ETHICS APPROVAL AND CONSENT TO PARTICIPATE

The study protocol has been approved by the Ethics Committee of Shandong Cancer Hospital (SDTHEC2020001013). The animal study was carried out in compliance with the guidance suggestion of Animal Care Committee of Shandong Cancer Hospital.

CONSENT FOR PUBLICATION

Not applicable.

ORCID

Zhaoyun Liu https://orcid.org/0000-0003-2966-3564
Zhiyong Yu https://orcid.org/0000-0002-2569-9458
Dawei Chen https://orcid.org/0000-0002-6762-7997
Meng Wu https://orcid.org/0000-0003-3213-2967
Jinming Yu https://orcid.org/0000-0001-5933-9912

REFERENCES

1. Wisdom AJ, Mowery YM, Hong CS, Himes JE, Nabet BY, Qin X, et al. Single cell analysis reveals distinct immune landscapes in transplant and primary sarcomas that determine response or resistance to immunotherapy. Nat Commun. 2020;11(1):6410.

2. Weichselbaum RR, Liang H, Deng L, Fu YX. Radiotherapy and immunotherapy: a beneficial liaison? Nat Rev Clin Oncol. 2017;14(6):365-79.
3. Rodriguez-Ruiz ME, Vanpouille-Box C, Melero I, Formenti SC, Demaria S. Immunological Mechanisms Responsible for Radiation-Induced Abscopal Effect. Trends Immunol. 2018;39(8):644-55.
4. Ngwa W, Irabor OC, Schoenfeld JD, Hesser J, Demaria S, Formenti SC. Using immunotherapy to boost the abscopal effect. Nat Rev Cancer. 2018;18(5):313-22.
5. Schnell A, Bod L, Madi A, Kuchroo VK. The yin and yang of co-inhibitory receptors: toward anti-tumor immunity without autoimmunity. Cell Res. 2020;30(4):285-99.
6. Wang Y, Wang M, Wu HX, Xu RH. Advancing to the era of cancer immunotherapy. Cancer Commun (Lond). 2021;41(9):803-29.
7. Zhang M, Yang W, Wang P, Deng Y, Dong YT, Liu FF, et al. CCL7 recruits cDC1 to promote antitumor immunity and facilitate checkpoint immunotherapy to non-small cell lung cancer. Nat Commun. 2020;11(1):6119.
8. Chen D, Barsoumian HB, Yang L, Younes AI, Verma V, Hu Y, et al. SHP-2 and PD-L1 Inhibition Combined with Radiotherapy Enhances Systemic Antitumor Effects in an Anti-PD-1-Resistant Model of Non-Small Cell Lung Cancer. Cancer Immunol Res. 2020;8(7):883-94.
9. Shang S, Liu J, Verma V, Wu M, Welsh J, Yu J, et al. Combined treatment of non-small cell lung cancer using radiotherapy and immunotherapy: challenges and updates. Cancer Commun (Lond). 2021;41(11):1086-99.
10. McLaughlin M, Patin EC, Pedersen M, Wilkins A, Dillon MT, Melcher AA, et al. Inflammatory microenvironment remodelling by tumour cells after radiotherapy. Nat Rev Cancer. 2020;20(4):203-17.
11. Zhang W, Yan C, Gao X, Li X, Cao F, Zhao G, et al. Safety and Feasibility of Radiotherapy Plus Camrelizumab for Locally Advanced Esophageal Squamous Cell Carcinoma. Oncologist. 2021;26(7):e1110-e24.
12. Saxena V, Li L, Paluskievicz C, Kasinath V, Bean A, Abdi R, et al. Role of lymph node stroma and microenvironment in T cell tolerance. Immunol Rev. 2019;292(1):9-23.
13. Druzd D, Matveeva O, Ince L, Harrison U, He W, Schmal C, et al. Lymphocyte Circadian Clocks Control Lymph Node Trafficking and Adaptive Immune Responses. Immunity. 2017;46(1):120-32.
14. Gasteiger G, Ataide M, Kastenmuller W. Lymph node - an organ for T-cell activation and pathogen defense. Immunol Rev. 2016;271(1):200-20.
15. Liang H, Deng L, Hou Y, Meng X, Huang X, Rao E, et al. Host STING-dependent MDSC mobilization drives extrinsic radiation resistance. Nat Commun. 2017;8(1):1736.
16. Yang Y, Wu M, Cao D, Yang C, Jin J, Wu L, et al. ZBP1-MLKL necroptotic signaling potentiates radiation-induced antitumor immunity via intratumoral STING pathway activation. Sci Adv. 2021;7(41):eabf6290.
17. Buchwald ZS, Nasti TH, Lee J, Eberhardt CS, Wieland A, Im SJ, et al. Tumor-draining lymph node is important for a robust abscopal effect stimulated by radiotherapy. J Immunother Cancer. 2020;8(2).
18. Chen M, Qiao G, Hylander BL, Mohammadpour H, Wang XY, Subjeck JR, et al. Adrenergic stress constrains the development of anti-tumor immunity and abscopal responses following local radiation. Nat Commun. 2020;11(1):1821.
19. Dammeijer F, van Gulijk M, Mulder EE, Lukkes M, Klaase L, van den Bosch T, et al. The PD-1/PD-L1-Checkpoint Restrains T cell Immunity in Tumor-Draining Lymph Nodes. Cancer Cell. 2020;38(5):685-700.e8.
20. Takeshima T, Chamoto K, Wakita D, Ohkuri T, Togashi Y, Shirato H, et al. Local radiation therapy inhibits tumor growth through the generation of tumor-specific CTL: its potentiation by combination with Th1 cell therapy. Cancer Res. 2010;70(7):2697-706.
21. Marciscano AE, Ghasemzadeh A, Nirschl TR, Theodros D, Kochel CM, Francica BJ, et al. Elective Nodal Irradiation Attenuates the Combinatorial Efficacy of Stereotactic Radiation Therapy and Immunotherapy. Clin Cancer Res. 2018;24(20):5058-71.
22. Fransen MF, Schoonderwoerd M, Knopf P, Camps MG, Hawinkels LJ, Kneilling M, et al. Tumor-draining lymph nodes are pivotal in PD-1/PD-L1 checkpoint therapy. JCI Insight. 2018;3(23).
23. Liu Y, Dong Y, Kong L, Shi F, Zhu H, Yu J. Abscopal effect of radiotherapy combined with immune checkpoint inhibitors. J Hematol Oncol. 2018;11(1):104.
24. Lippert TP, Greenberg RA. The abscopal effect: a sense of DNA damage is in the air. J Clin Invest. 2021;131(9).
25. Dudzinski SO, Cameron BD, Wang J, Rathmell JC, Giorgio TD, Kirschner AN. Combination immunotherapy and radiotherapy causes an abscopal treatment response in a mouse model of castration resistant prostate cancer. J Immunother Cancer. 2019;7(1):218.
26. Brooks ED, Chang JY. Time to abandon single-site irradiation for inducing abscopal effects. Nat Rev Clin Oncol. 2019;16(2):123-35.
27. Zhang X, Niedermann G. Abscopal Effects With Hypofractionated Schedules Extending Into the Effector Phase of the Tumor-Specific T-Cell Response. Int J Radiat Oncol Biol Phys. 2018;101(1):63-73.
28. Kim GB, Sung HD, Nam GH, Kim W, Kim S, Kang D, et al. Design of PD-1-decorated nanocages targeting tumor-draining lymph node for promoting T cell activation. J Control Release. 2021;333:328-38.
29. Im SJ, Hashimoto M, Gerner MY, Lee J, Kissick HT, Burger MC, et al. Defining CD8+ T cells that provide the proliferative burst after PD-1 therapy. Nature. 2016;537(7620):417-21.
30. van Pul KM, Fransen MF, van de Ven R, de Gruijl TD. Immunotherapy Goes Local: The Central Role of Lymph Nodes in Driving Tumor Infiltration and Efficacy. Front Immunol. 2021;12:643291.
31. Hinson AM, Massoll NA, Jolly LA, Stack BC, Jr., Bodenner DL, Franco AT. Structural alterations in tumor-draining lymph nodes before papillary thyroid carcinoma metastasis. Head Neck. 2017;39(8):1639-46.
32. Spranger S, Koblish HK, Horton B, Scherle PA, Newton R, Gajewski TF. Mechanism of tumor rejection with doublets of CTLA-4, PD-1/PD-L1, or IDO blockade involves restored IL-2 production and proliferation of CD8(+) T cells directly within the tumor microenvironment. J Immunother Cancer. 2014;2:3.
33. Sharabi AB, Nirschl CJ, Kochel CM, Nirschl TR, Francica BJ, Velarde E, et al. Stereotactic Radiation Therapy Augments

Antigen-Specific PD-1-Mediated Antitumor Immune Responses via Cross-Presentation of Tumor Antigen. Cancer Immunol Res. 2015;3(4):345-55.
34. Blankenstein T, Coulie PG, Gilboa E, Jaffee EM. The determinants of tumour immunogenicity. Nat Rev Cancer. 2012;12(4):307-13.
35. Fan JB, Miyauchi S, Xu HZ, Liu D, Kim LJY, Burkart C, et al. Type I Interferon Regulates a Coordinated Gene Network to Enhance Cytotoxic T Cell-Mediated Tumor Killing. Cancer Discov. 2020;10(3):382-93.
36. Lee JY, Hall JA, Kroehling L, Wu L, Najar T, Nguyen HH, et al. Serum Amyloid A Proteins Induce Pathogenic Th17 Cells and Promote Inflammatory Disease. Cell. 2020;180(1): 79-91.e16.
37. Abdulrahman Z, Santegoets SJ, Sturm G, Charoentong P, Ijsselsteijn ME, Somarakis A, et al. Tumor-specific T cells support chemokine-driven spatial organization of intratumoral immune microaggregates needed for long survival. J Immunother Cancer. 2022;10(2).
38. Goodall KJ, Nguyen A, Andrews DM, Sullivan LC. Ribosylation of the CD8alphabeta heterodimer permits binding of the nonclassical major histocompatibility molecule, H2-Q10. J Biol Chem. 2021;297(4):101141.
39. Jansen CS, Prokhnevska N, Master VA, Sanda MG, Carlisle JW, Bilen MA, et al. An intra-tumoral niche maintains and differentiates stem-like CD8 T cells. Nature. 2019;576(7787): 465-70.
40. Krishna S, Lowery FJ, Copeland AR, Bahadiroglu E, Mukherjee R, Jia L, et al. Stem-like CD8 T cells mediate response of adoptive cell immunotherapy against human cancer. Science. 2020;370(6522):1328-34.
41. Chen Y, Zhang S, Wang Q, Zhang X. Tumor-recruited M2 macrophages promote gastric and breast cancer metastasis via M2 macrophage-secreted CHI3L1 protein. J Hematol Oncol. 2017;10(1):36.
42. Rawji KS, Young AMH, Ghosh T, Michaels NJ, Mirzaei R, Kappen J, et al. Niacin-mediated rejuvenation of macrophage/microglia enhances remyelination of the aging central nervous system. Acta Neuropathol. 2020;139(5): 893-909.
43. Wei J, Montalvo-Ortiz W, Yu L, Krasco A, Ebstein S, Cortez C, et al. Sequence of alphaPD-1 relative to local tumor irradiation determines the induction of abscopal antitumor immune responses. Sci Immunol. 2021;6(58).
44. Kohlhapp FJ, Broucek JR, Hughes T, Huelsmann EJ, Lusciks J, Zayas JP, et al. NK cells and CD8+ T cells cooperate to improve therapeutic responses in melanoma treated with interleukin-2 (IL-2) and CTLA-4 blockade. J Immunother Cancer. 2015;3:18.
45. Sunshine JC, Perica K, Schneck JP, Green JJ. Particle shape dependence of CD8+ T cell activation by artificial antigen presenting cells. Biomaterials. 2014;35(1):269-77.
46. Ramesh P, Shivde R, Jaishankar D, Saleiro D, Le Poole IC. A Palette of Cytokines to Measure Anti-Tumor Efficacy of T Cell-Based Therapeutics. Cancers (Basel). 2021;13(4).
47. Galli F, Aguilera JV, Palermo B, Markovic SN, Nistico P, Signore A. Relevance of immune cell and tumor microenvironment imaging in the new era of immunotherapy. J Exp Clin Cancer Res. 2020;39(1):89.
48. Helmink BA, Reddy SM, Gao J, Zhang S, Basar R, Thakur R, et al. B cells and tertiary lymphoid structures promote immunotherapy response. Nature. 2020;577(7791):549-55.
49. Xiang X, Wang J, Lu D, Xu X. Targeting tumor-associated macrophages to synergize tumor immunotherapy. Signal Transduct Target Ther. 2021;6(1):75.

SUPPORTING INFORMATION

Additional supporting information can be found online in the Supporting Information section at the end of this article.

How to cite this article: Liu Z, Yu Z, Chen D, Verma V, Yuan C, Wang M, et al. Pivotal roles of tumor-draining lymph nodes in the abscopal effects from combined immunotherapy and radiotherapy. Cancer Commun. 2022;1–16.
https://doi.org/10.1002/cac2.12348